



Effect of Anodizing Process on Inter Laminar Shear Strength of GLARE Composite through T-Peel Test: Experimental and Numerical Approach

M.Y. Khalid¹ · A. Al Rashid² · M.F. Sheikh¹

Received: 24 July 2020 / Accepted: 23 December 2020 / Published online: 26 January 2021
© The Society for Experimental Mechanics, Inc 2021, corrected publication 2021

Abstract

Glass laminate aluminum reinforced epoxy (GLARE) is a vital class fiber metal laminates (FMLs) and advanced aircraft material. Despite the ongoing research and utilization of FMLs in applications like structures and aircraft, the weakness is particularly the materials' delamination. This phenomenon is still observed as the primary confinement for an increased and efficient utilization of the materials. In this study, interlaminar shear strength (ILSS) of GLARE composite is improved through many chemical treatments and the anodizing process. T-peel test characterizes the ILSS through the ASTM D1876–08 standard. The numerical model was also developed to predict the ILSS of GLARE laminates and their performance. Results show that the anodizing process enhances the ILSS of GLARE composite. Anodizing makes the aluminium surface porous and improves glass fiber's adhesion with Aluminium surface. The numerical models successfully predict experimental results for un-anodized samples.

Keywords FML · GLARE · T-peel Test · Simulation · VARTM

Introduction

The world is shifting towards lightweight materials due to many problems adhered due to the weight of automobiles. Composite materials and advanced manufacturing techniques were introduced in cars, aircraft, and aerospace industry to solve this problem [1–3]. Fiber metal laminates (FML) is a new class of composite materials [4], are extensively used in aviation and defense applications because of their high strength to weight ratio. This new class of material joins the best features of fiberreinforced composites and metals. It has been generally viewed as a group of higher fatigue and damage resistance. Also, they have excellent damping and protection properties. There are three types of Fiber Metal

Laminates, GLARE, ARRAL, and CARALL [5, 6]. Their construction is so that glass, aramid, and carbon fibers are embedded between aluminium layers with the help of different resins. (ARRAL) For the most part, they are created for their application in airplane parts where fatigue resistance is essential, such as the lower wing and upper fuselage skins of an airplane [7].

Joining two materials to get a superior exhibition like that of the singles is a general objective [8] in FML design. Therefore, a good understanding of the adhesive layer properties is basic to predict the structural response of GLARE aircraft panels [9]. Interlaminar shear strength (ILSS) of FML can be determined in many ways [10]. Still, the T-peel test is an effective way to calculate ILSS because it efficiently involves large adherend deflections and strains compared to other ILSS test methods [11].

Finite Element Analysis (FEA) simulations [12] are widely used for predicting different mechanical properties of metal alloys and composites, including FML many researchers [13–15]. Cláudio S. Lopes et al. [16] explained the effects of porosity on the interlaminar shear strength of GLARE composite through a numerical approach. The definitive agreement was found between the ILSS test result and numerical simulation.

F. Khan et al. [13] investigated the effect of chemical and mechanical treatments on CARALL laminates through the t-peel test, according to ASTM D1876 standard. Specimens

✉ M.Y. Khalid
yasirkhalid94@gmail.com

✉ A. Al Rashid
anrashid@hbku.edu.qa

¹ Department of Mechanical Engineering, University of Management & Technology Lahore, Sialkot Campus, Punjab 51040, Pakistan

² Division of Sustainable Development, College of Science and Engineering, Hamad Bin Khalifa University, Qatar Foundation, Doha, Qatar



were prepared through Vacuum Assisted Resin Transfer Molding (VARTM) technique. A numerical simulation was also performed. Results showed that numerical simulation successfully predicts the delamination behavior of CARALL laminates. In another work [17], a similar type of chemical treatment was performed on ARALL laminates. Results explained that the effect of chemical treatment increased the mechanical properties of ARALL laminates.

R. G. J. VAN ROOIJEN et al. [18] studied the effects of chemical and mechanical pre-treatments on FML. Results indicated that the reinforced sheet's interface strength and properties play significant importance in the peel strength. Notably, due to the bonded sheet's deformation, it isn't easy to compare the peel strengths of specimens with different sheet thicknesses.

Tomasz Trzepiecinski et al. [19] compared the strength of different kinds of (FMLs), with an alternate method for setting up the adhesive coupling among aluminum alloy sheets and a polymer/fiber layer through peel test. It was found by adding an adhesive coupling; there was a notable increase in the laminate's peel strength. This noteworthy increase in the FML peel strength was possible due to the additional adhesive film's increased cost by 20%.

In another study, peel test adhesion quality of FML bonded joints was studied under salt spray aging conditions. The Peel test effectively evaluated the interface adhesion in different salty and non-salty aging conditions. Therefore, it can be utilized as a quick, dependable, and straightforward test to consider the drawn-out strength in the event of composite-metal reinforced joints [20].

Extensive investigation of GLARE with fatigue cracks and through cracks was performed by the authors [21–23]. As a result, from a preliminary investigation on notches, it appeared that notch strength highly depended on the number of cut fibers due to the production of holes (for fasteners, e.g.). The most extensive damage would result from a sharp notch like a through the thickness crack. In aluminium, this could result from a foreign object penetration as well as from fatigue. In the case of GLARE, fatigue

would not lead to through the thickness cracks. It could be concluded that the residual strength of Glare with fatigue cracks was considerably higher than that with cracks.

Shear load in an airplane fuselage will happen because of bending and torsion. Therefore, ILSS is likewise a significant parameter as the material isn't permitted to deform plastically beneath the limit load. The shear modulus and shear yield strength of different GLARE laminates are just about half of the solid 2024-T3 aluminium alloy. Undoubtedly, more work is expected to be done on the shear response of GLARE composite [24].

This research work is inspired by previous studies [13, 17]. It describes all the procedures to fabricate the GLARE composites and testing the specimens by keeping interfacial bonding strength. Samples were prepared through the VARTM technique. Two types of specimens are manufactured to compare and check the aluminium sheets and glass fiber's interfacial bonding. The two classifications were made by cleaning processes/chemical treatments on aluminium sheets, anodized aluminium sheets, and un-anodized aluminium sheets. After fabrication specimens were cut accordingly to ASTM D1876–08 standard.

Experimental Work

Materials

The general mechanical properties of consumed materials are discussed in Table 1.

Aluminium alloy 2024 T3

For the fabrication of GLARE composites, the Aluminium Alloys 2XXX series are used. The aluminium alloy series 2XXX contains elements Copper (Cu) and Magnesium (Mg) as their primary component. In this research, Aluminium Alloy 2024 T3 is used. The aluminium alloys

Table 1 Mechanical Properties of Consumed Materials

| Mechanical Properties | Consumed Materials | | |
|-----------------------|------------------------|-----------------------|------------------------------------|
| | Al 2024-T3 | S-Glass Fiber [13] | Araldite LY 5052/ Aradur 5052 [13] |
| Tensile Strength | 480 MPa | 335 MPa | 49–71 MPa |
| Tensile Modulus | 71 GPa | 19 GPa | 3.4 GPa |
| Melting Point | 500 °C | 1056 °C | – |
| Elongation | 10–15% | 4.82% | 1.5–2.5% |
| Poisson's Ratio | 0.33 | 0.2 | 0.35 |
| Density | 2.78 g/cm ³ | 2.5 g/cm ³ | 1.17 g/cm ³ |
| Thickness | 0.8 mm | 0.204 mm | – |
| Grade | H12 | 2*2-twill weave | Aerospace (Huntsman) |



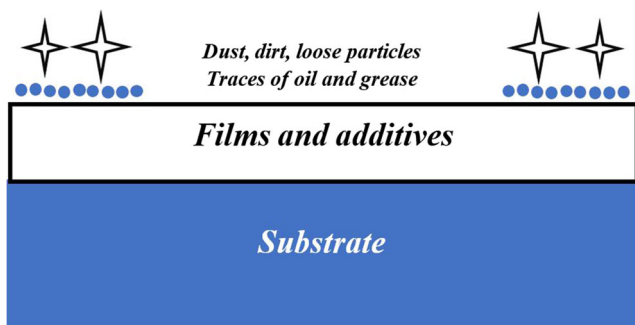


Fig. 1 The typical surface of aluminium 2024 T3

2XXX shows excellent fatigue properties, and due to this property, aluminium 2024 is widely used in the aerospace industry. 2024 alloy is offered in mostly heat-treated forms. Arrangement heat treatment involves three stages; warming to a particular temperature, drenching for quite a while, and quickly extinguishing. The surface of aluminium 2024 T3 after heat treatment is shown in Fig. 1 In this study, a sheet thickness of 0.8 mm is used.

Glass fiber S2

In this study, the S2 Glass Fiber is used. As compared to conventional glass fibers, the improved properties of S-2 Glass fibers result in better weight performance and strength to weight ratio. Compared to aramid and carbon fibers, S-2 Glass fibers’ enhanced properties give better cost performance [25].

Adhesive system

In this study, Araldite LY5052 epoxy resin and Aradur 5052 hardener used as an adhesion system to bond aluminium layers with glass fiber; the two constituents are

epoxy resin and the hardener. Its primary applications are in aerospace and composites, tooling, and aircraft repair. It has low viscosity and easy impregnation of reinforcement materials. It has High-temperature resistance (glass transition temperature) after ambient cure: 60 °C, after post-cure at 100:120 °C. Additionally, overlays show extraordinary mechanical and element properties. This framework is qualified by the Luftfahrtbundesamt (German Aircraft Authority) for the generation of light-weight flyers.

All the cleaning dimensions of aluminium 2024 was 2 in. (50.8 mm) by 10 in. (254). These sheets/strips were obtained from the original aluminium sheet and shear cutter machine.

Surface Preparation

For proper bonding and good adhesion, removing grease, dust particles, and other contamination types is necessary. So, the surface was prepared through both mechanical and electrochemical processes.

Mechanical treatment

The aluminium sheets and glass fiber, first aluminium 2024 alloy is treated mechanically using abrasion for better bonding. Sandpapers of grades 800C, 1200C, and 1500C are used for this purpose. The primary purpose of using sandpaper is to rough the surface for better bonding. Further chemical treatments were applied to the aluminium sheets for better surface treatments.

Anodizing process

Anodizing is an electrochemical process that converts the metal surface into a decorative, durable, corrosion-resistant,

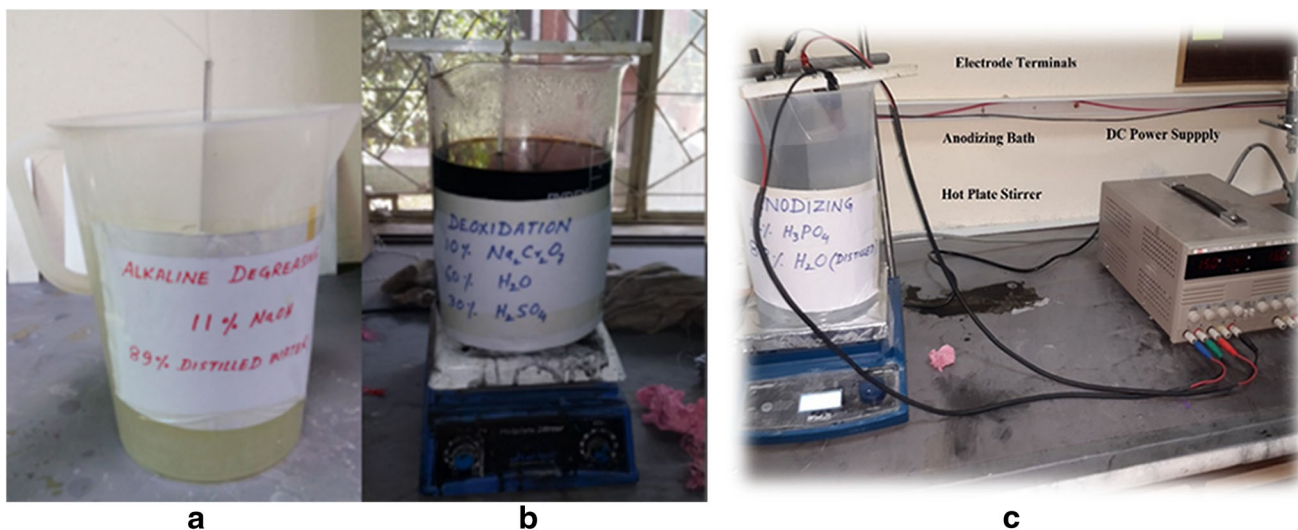
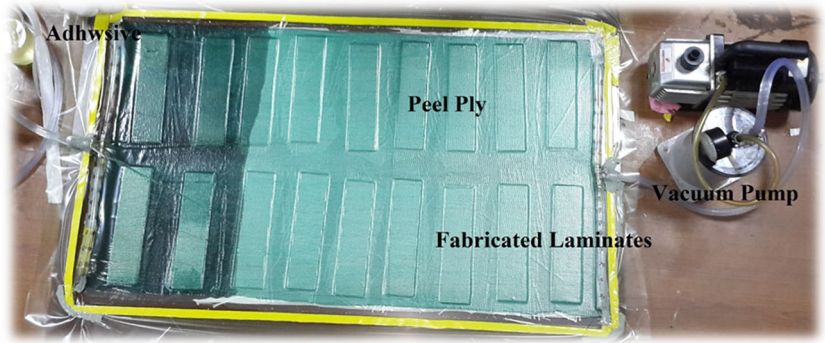


Fig. 2. (a). Alkaline Degreasing Solution. (b). Deoxidation Solution. (c). Anodizing

Fig. 3 VARTM Process



anodic oxide finish [11]. Aluminum is ideal for anodizing, although other nonferrous metals, such as magnesium and titanium, can also be anodized. The purpose of anodizing is to produce a porous oxide layer, which gives better interfacial bonding. Two types of layers, porous and barrier, are produced on the surface with a compatible electrolyte. Before anodizing the aluminium sheets, the following cleaning processes were done.

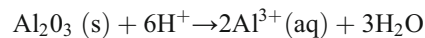
Alkaline degreasing

Alkaline degreasing is a pre-treatment process for metals before using for different purposes where a clean metal surface is required. This process profoundly cleans the metal part from all types of oils, waxes, and greases. It also tends other contaminants to stick on the surface of metals after machining. For this purpose, a solution of 11% NaOH (Sodium Hydroxide) and 89% distilled water was prepared and mixed to make a proper solution. Then aluminium sheets are dipped in the NaOH solution for 10 min and then washed with distilled water; it gives a much better surface free of grease and dust particles. Fig. 2a shows alkaline degreasing.

Deoxidation

The primary purpose of deoxidation is to remove the aluminium oxide layer from the aluminium sheet’s surface. In this process, the pure aluminium surface is obtained. A

de-oxidant solution containing 10% by weight Sodium Dichromate, 30% by weight Sulphuric acid, and 60% by weight distilled water were prepared for deoxidation. The aluminium strips were dipped in the hot solution, which maintains the temperature of 80 °C for 15 min. The Deoxidation process is shown in Fig. 2b. The following reaction takes place:



Anodizing

The anodizing was done according to ASTM D3993 standard. After alkaline degreasing and deoxidation, now pure aluminium surface was obtained, which is readily anodizing. An anodizing solution contains 12% by weight Phosphoric acid, and 88% by weight distilled water was prepared. The Al sheets were then dipped in the anodizing solution, the sheets were given an anode supply where the

Table 2 Specimens chemical treatment scheme and their description

| Sr. No. | Stacking Scheme | Mechanical treatment | Chemical Treatment | Anodizing | CODE/Description |
|---------|-----------------|----------------------|--------------------|-----------|------------------|
| 1 | Al/Glass/Al | yes | yes | yes | A-GLARE |
| 2 | | yes | yes | no | UA-GLARE |

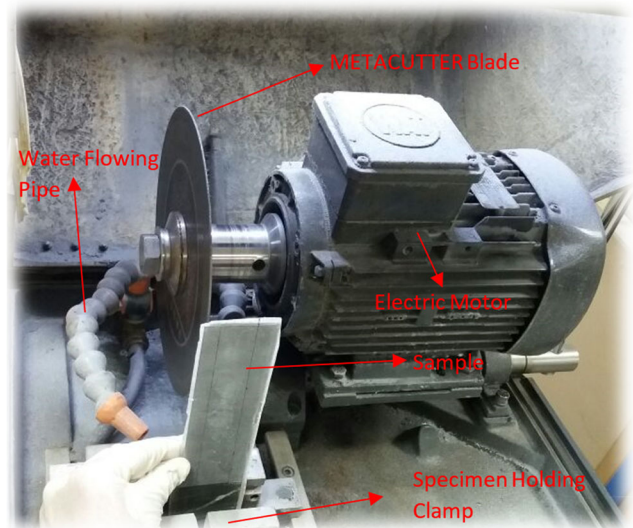


Fig. 4 META Cutter Machine

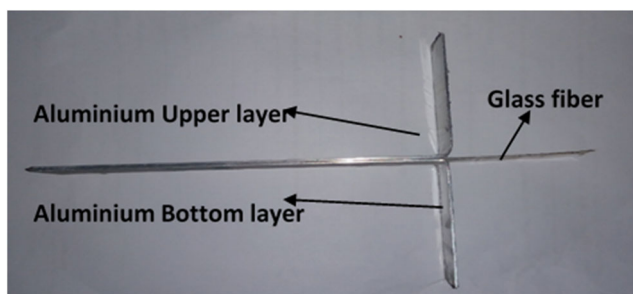


Fig. 5 T-Peel GLARE specimen

stainless sheet is provided the cathode supply, and a voltage of 12 V is applied for 25 min. After this, Al sheets/strips were covered; this is done to account for the oxide layer's effect, so this layer cannot take part in any environmental chemical reaction. Fig. 2c shows the final anodizing process on aluminium alloy 2024 T3.

Samples Preparations

As discussed earlier, the samples were prepared according to the VARTM process. The glass mold is prepared and cleaned with acetone's help to remove the dust and grease particles on the mold surface in the first step. Typically wax or spray of silicon is done below or at the bottom surface of the glass mold, and then a piece of peel ply was laid upon the glass mold, which helps remove the fabricated parts. Peel ply is a porous fabric; then, the aluminium 2024 T3 sheets were laid in such a manner that at the bottom, one aluminium sheet, then Glass fiber, and then an aluminium sheet. The system built top peel ply was again placed and then flow medium, net-type meshed sheet. This sheet helps the resin flow along the length and thickness. The spiral pipe is placed at both ends to

create a vacuum from one side and the flow of resin from the other side. After making this arrangement, a vacuum bag is laid and make it airtight with tacky tapes. The vacuum pump action is applied to one side and epoxy on the other side; when the epoxy valve opens, the epoxy starts flowing through the entire setup. After completing the resin's infiltration, both inlets and outlets' opening and closing ends were sealed so that no air will enter inside the system. This VARTM process is shown in fig. 3. The curing of specimens was taking place for 48 h at 23 °C.

The fiber volume fraction in these composites was approximately 30%. The thickness on GLARE specimens was 2 mm; this fabricated part consists of two aluminium sheets of 0.5 mm, a Glass fiber S2 layer, and a reinforced composite of 1 mm thickness. Two types of specimens were fabricated, one with anodized aluminium sheets and one with unanodized aluminium sheets using the VARTM process, as discussed in Table 2. Now there are two sets of samples ready for T-peel testes.

Mechanical Testing

As discussed earlier, the specimens were cut according to the ASTM D1876–08 standard. T-peel tests were performed on MTS 810 (Material Testing Machine). The original dimensions of the laminates were 2 in. by 10 in.. But for achieving T-peel standard measurements, the samples of anodized and non-anodized are cut on Meta-Cut cutting machine with final dimensions of 1-in. (25 mm) by 9 (228.6 mm) inches. Both lengths, i.e., bonded length 177 mm and t-peel length 50 mm, are included. The cross-head speed was 5in/min. The METACUT machine, as shown in Fig. 4. The one end

Fig. 6. (a). Force vs. Displacement Curve for UA-sample. (b). Force vs. Time Curve for UA-sample

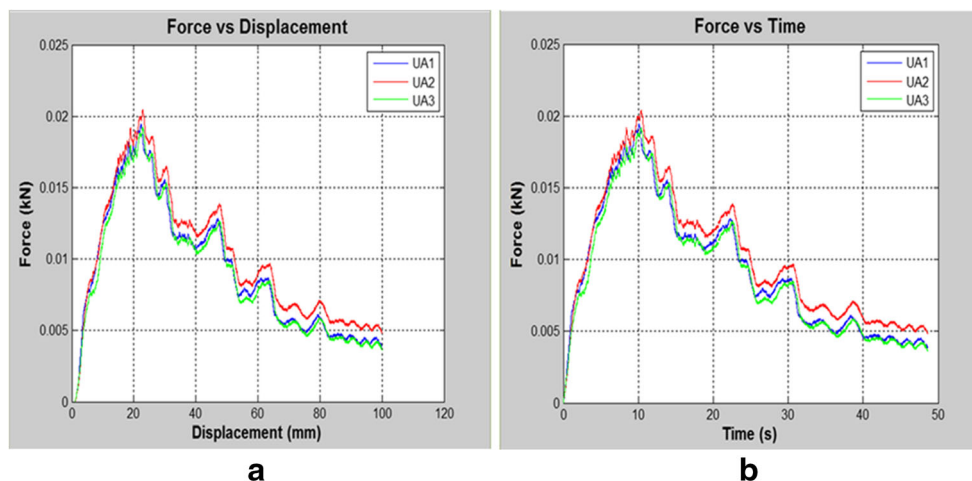
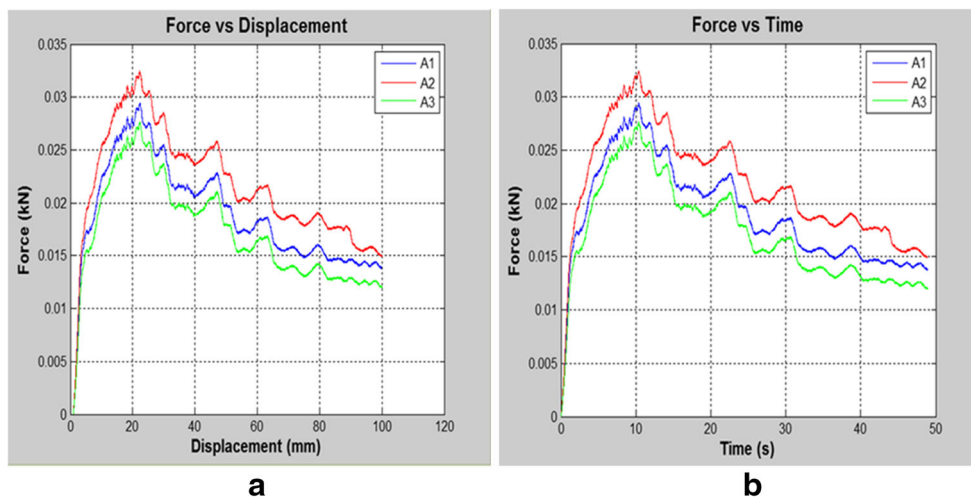


Fig. 7. (a). Force vs. Displacement Curve for A-sample. (b). Force vs. Time Curve for A-sample



of the laminates is peeled off with the dimension of one inch and bent to about 90 degrees for an easy grip in the machine fixture. The t-peel specimen is shown in Fig. 5.

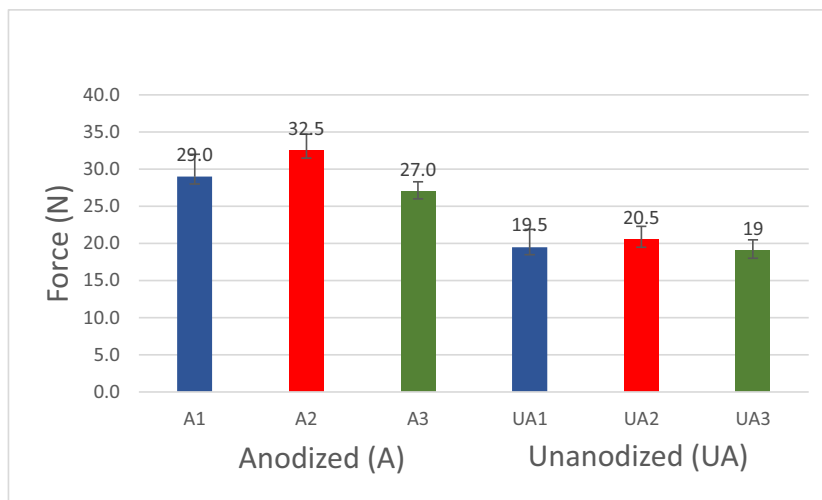
Results and Discussion

The force vs. displacement and force vs. time curves for un-anodized and anodized samples are shown in Figs. 6 and 7. The anodizing technique on GLARE composite enhanced its mechanical properties [26, 27]. The average maximum force for the un-anodized sample was 19.56 N, where for the anodized sample, 29.56 N were obtained. Clearly, ILSS strength is increased.

From the curves, it can be easily identified three zones of curves. That is the pre-initial zone, initial zone, and stable zone. The bar charts for the maximum load is shown in Fig. 8 for both specimens. The

anodized samples A1, A2, and A3, have good interfacial bonding, and it required more force to peel off while the peak loads of un-anodized UA1, UA2, and UA3 show that they needed less force to peel off. Therefore, anodized specimens have good interlaminar shear strength. Figure 9 shows the visual inspection of both samples' results after T-peel tests. Figure 9 shows that the GLARE specimens with anodized aluminium 2024 T3 alloy have excellent interfacial bonding between Glass fabric and Aluminium sheets. The peeled surface has some fiber stick on the surface. While observing the specimens fabricated with un-anodized aluminium 2024, T3 alloy has low interfacial bonding, and the peel strength is less than anodized samples. The surface peel is evident and has no adhesive particles or fabric particles stick. Similar results were reported in the previous study [13, 17] for CARALL and ARALL laminates.

Fig. 8 Comparison of Maximum Force for different samples



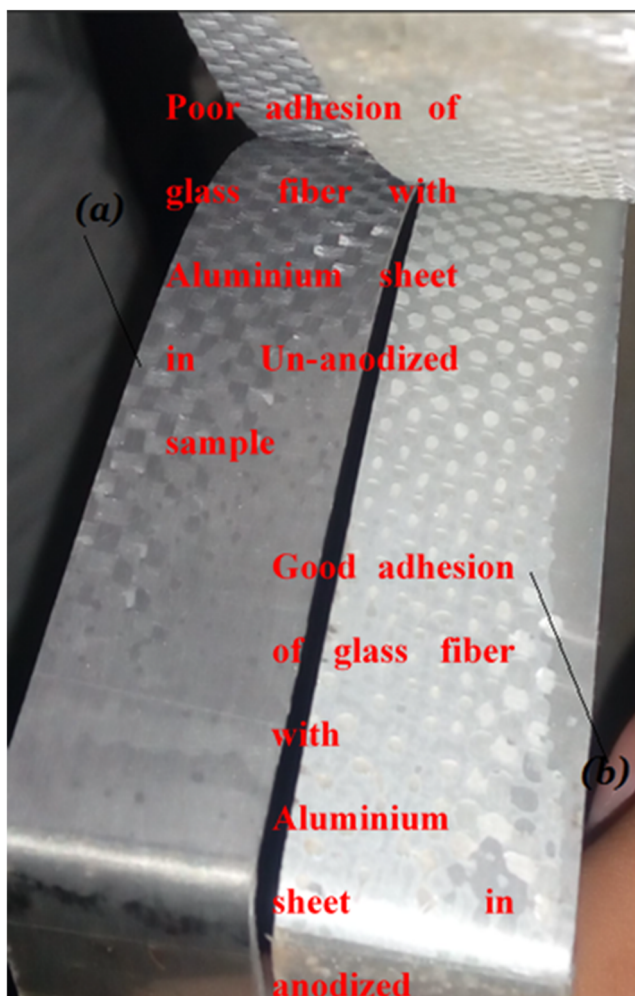


Fig. 9 Visual Inspection of both Samples

Numerical Simulations

The T-peel test’s numerical simulation was done on ABAQUS software [28] for the GLARE specimen. The finite element method model contains a 2D plain stress

double cantilever beam. Three Components use in this simulation with the displacement as an input parameter. The top part of the model was the Aluminium sheet; the bottom is the glass fiber and epoxy between glass and Aluminium. The dimensions of the model are the same as in the experiment. The mechanical properties of Aluminium 2024 alloy, glass fiber, and epoxy resin used in this simulation were taken from Table 1. The glass fiber layer’s motion is constrained in the *x*-Axis *axis* motion, where the Aluminum layer is free on the *y*-axis. Aluminium and glass fiber are then assembled by using an instance command. Create surfaces between Aluminium, glass, and epoxy. These Surfaces were created in ABAQUS to define the purpose of bonding between them. If the two surfaces are to be joined together, one is called the master surface, and the other is called the slave surface. These surfaces have properties such as adhesiveness or cohesiveness. Each part was meshed to convert into discrete nodes to get accurate results. The model has independently meshed parts. Aluminium and glass epoxy laminates were meshed using a structured quadratic, plane stress element. The adhesive was meshed using a sweep quadratic (when the sweep path was upward). After part meshing, edit mesh and assigned zero thickness for cohesive elements. Apply boundary conditions on aluminium, which can only move in the *y*-axis, and on the glass fiber, which is fixed. The first boundary condition was applied on the bottom side of glass fiber using the initial step, restrict this side for any type of displacement.

The displacement in the laminate by the applications of strain is shown in Fig. 10. Figure 10 shows that the aluminium sheet’s point starts peeling from has a maximum displacement of 10 mm and starts decreasing gradually till the tip of laminate -0.0003 mm. Figure 11 shows the reaction force along the *Y*-axis. It is taken as the output. The resulting force developed in delaminating the specimen is 20 N and is the same for un-anodized tested samples.

Fig. 10 Displacement in the Laminate in ABAQUS

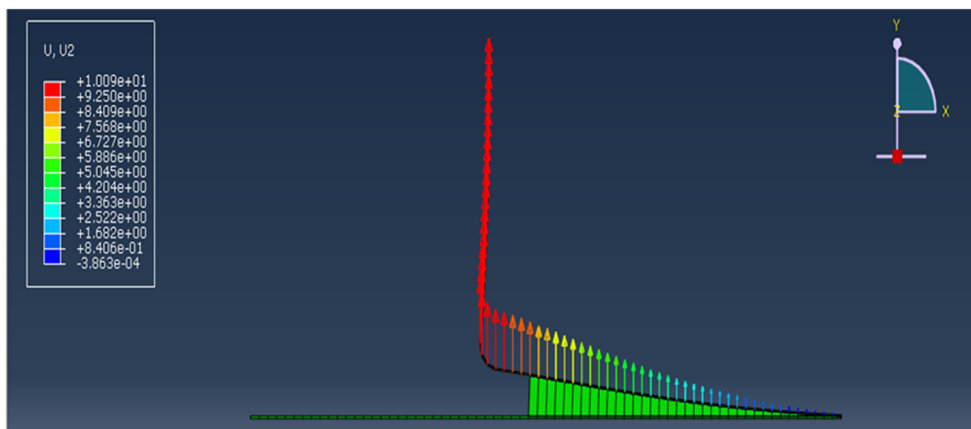
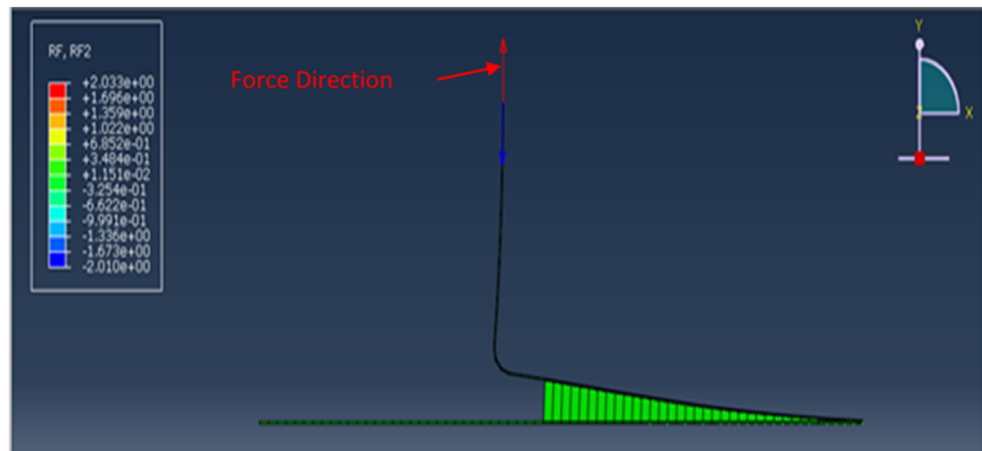


Fig. 11 Maximum Force of Laminate in ABAQUS



Conclusions

In this study, the interlaminar shear strength of GLARE composite is studied through different chemical and mechanical treatments. It is observed that the anodizing process increases the interfacial bonding between aluminium sheets and glass fiber. The effect of anodizing acts creates a porous surface at aluminium sheets, and the resin sticks tightly between glass fiber and aluminium. T-peel tests showed that GLARE composites' strength could be enhanced easily by the VARTM process, which is very cheap and easy to establish. Comparing the results between the two sets of specimens that are anodized and un-anodized shows that the anodized samples give a better result. So, GLARE composite ILSS easily be enhanced through the mechanical, chemical, and electrochemical processes on aluminium alloys. The numerical simulation was successfully performed on ABAQUS reported results of simulation exactly matched with un-anodized sample results. However, these simulation results were less than that of anodized samples because it is challenging to create a porous surface concept on Aluminium due to the anodizing process in software.

There are now many treatments like coupling agent techniques (silane or sol-gel) and other dry surface techniques (Cold Plasma) available for GLARE laminates. In the future, it is recommended ILSS should be measured under these techniques. Also, more time should be given in the anodizing process, which makes the surface more porous, and hence results will be in strong interfacial bonding. One of the challenges with the current FEA-based study is that it captures only the ILSS strength of GLARE composite; however, GLARE laminates' fracture energy can be evaluated through FEA in the future.

References

1. Marissen, R. (1989). Mechanical aspects related to fibre fracture in ARALL[®] 2 laminates. In *Advances in Fatigue Sci. Technol.* (pp. 697–707). Springer, Dordrecht.
2. Mouritz, A. P., Gellert, E., Burchill, P., & Challis, K. (2001). Review of advanced composite structures for naval ships and submarines. *Compos. Struct.* 53(1), 21–42.
3. Al Rashid A, Khan SA, Al-Ghamdi SG, Koç M (2020) Additive manufacturing: Technology, applications, markets, and opportunities for the built environment. *Autom Constr* 118:103268
4. Asundi A, Choi AY (1997) Fiber metal laminates: an advanced material for future aircraft. *J Mater Process Technol* 63(1–3):384–394
5. Sinmazçelik T, Avcu E, Bora MÖ, Çoban O (2011) A review: Fibre metal laminates, background, bonding types and applied test methods. *Mater Des* 32(7):3671–3685
6. Cantwell WJ (2000) The mechanical properties of fibre-metal laminates based on glass fibre reinforced polypropylene. *Compos Sci Technol* 60(7):1085–1094
7. Giasin K, Ayvar-Soberanis S, Hodzic A (2015) An experimental study on drilling of unidirectional GLARE fibre metal laminates. *Compos Struct* 133:794–808
8. Khalid MY, Nasir MA, Ali A, Al Rashid A, Khan MR (2020) Experimental and numerical characterization of tensile property of jute/carbon fabric reinforced epoxy hybrid composites. *SN Appl Sci* 2(4):1–10
9. Fedele R, Raka B, Hild F, Roux S (2009) Identification of adhesive properties in GLARE assemblies using digital image correlation. *J Mech Phys Solids* 57(7):1003–1016
10. Kotik HG, Ipiña JEP (2017) Short-beam shear fatigue behavior of fiber metal laminate (Glare). *Int J Fatigue* 95:236–242
11. Li Q, Batra RC, Graham I, Dillard DA (2019) Examining T-peel specimen bond length effects: Experimental and numerical explorations of transitions to steady-state debonding. *Int J Solids Struct* 180:72–83
12. Ali A, Nasir MA, Khalid MY, Nauman S, Shaker K, Khushnood S et al (2019) Experimental and numerical characterization of mechanical properties of carbon/jute fabric reinforced epoxy hybrid composites. *J Mech Sci Technol* 33(9):4217–4226
13. Khan F et al (2017) Effect of various surface preparation techniques on the delamination properties of vacuum infused Carbon fiber reinforced aluminum laminates (CARALL). *Experiment Numeric Simulat* 31(11):5265–5272
14. Kamocka M, Mania R J (2019, February) Numerical study of axially compressed FML profile including delamination. In: *AIP Conference Proceedings* (Vol. 2060, No. 1, p. 020003). AIP Publishing LLC
15. Al Rashid A, Imran R, Khalid MY (2020) Determination of opening stresses for railway steel under low cycle fatigue using digital image correlation. *Theor Appl Fract Mech* 108:102601

16. Lopes CS, Remmers JJ, Gürdal Z (2008) Influence of porosity on the interlaminar shear strength of fibre-metal laminates. *Key Eng Mater* 383:35–52. Trans Tech Publications Ltd
17. Qaiser H, Umar S, Nasir A, Shah M, Nauman S (2015) Optimization of interlaminar shear strength behavior of anodized and unanodized ARALL composites fabricated through VARTM process. *Int J Mater Form* 8(3):481–493
18. Van Rooijen RGJ, Sinke J, Van Der Zwaag S (2005) Improving the adhesion of thin stainless steel sheets for fibre metal laminate (FML) applications. *J Adhes Sci Technol* 19(16):1387–1396
19. Kubit A, Trzepieciński T, Krasowski B, Slota J, Spišák E (2020) Strength analysis of a rib-stiffened GLARE-based thin-walled structure. *Mater* 13(13):2929
20. de Freitas ST, Banea MD, Budhe S, de Barros S (2017) Interface adhesion assessment of composite-to-metal bonded joints under salt spray conditions using peel tests. *Compos Struct* 164:68–75
21. Alderliesten RC (2007) Analytical prediction model for fatigue crack propagation and delamination growth in Glare. *Int J Fatigue* 29(4):628–646
22. Alderliesten RC, Homan JJ (2006) Fatigue and damage tolerance issues of Glare in aircraft structures. *Int J Fatigue* 28(10):1116–1123
23. Shim DJ, Alderliesten RC, Spearing SM, Buriánek DA (2003) Fatigue crack growth prediction in GLARE hybrid laminates. *Compos Sci Technol* 63(12):1759–1767
24. Wu G, Yang JM (2005) The mechanical behavior of GLARE laminates for aircraft structures. *J Miner Metal Mater* 57(1):72–79
25. Kinsella M, Murray D, Crane D, Mancinelli J, Kranjc M (2001, November) Mechanical properties of polymeric composites reinforced with high strength glass fibers, vol 33. International SAMPE Technical Conference, pp 1644–1657
26. Yoon S, Jong W, Soap H, Kwon H (2010) Effects of surface pretreatment and void content on GLARE laminate process characteristics. *J Mater Process Tech* 210(8):1008–1016
27. Xu Y, Li H, Shen Y, Liu S, Wang W, Tao J (2016) Improvement of adhesion performance between aluminum alloy sheet and epoxy based on anodizing technique. *Int. J. Adhes. Adhes.* 70:74–80
28. Al Rashid A, Khalid MY, Imran R, Ali U, Koc M (2020) Utilization of banana fiber-reinforced hybrid composites in the sports industry. *Materials* 13(14):3167

Publisher's Note Springer Nature remains neutral with regard to jurisdictional claims in published maps and institutional affiliations.

